Pure Appl. Chem., Vol. 73, No. 1, pp. 17–22, 2001.

A glance into the bulk of solvent polymeric pH membranes*

Ernő Lindner[1,†], Robert E. Gyurcsányi[1,2], and Bradford D. Pendley[3]

[1]Joint Graduate Program in Biomedical Engineering, The University of Memphis and University of Tennessee Health Science Center, Herff College of Engineering, Memphis, TN 38152-6582, USA; [2]Research Group of Technical Analytical Chemistry of the Hungarian Academy of Sciences, Department of Analytical Chemistry, Budapest University of Technology and Economics, 1111 Budapest, Gellért tér 4, Hungary; [3]Department of Chemistry, Rhodes College, 2000 North Parkway, Memphis, TN 38112, USA

Abstract: The pH-sensitive chromoionophores brought the dream of the ion-selective membrane scientist close to realization. With the help of these molecules, one can build pH-sensitive, ion-selective electrodes and look into the bulk of solvent polymeric membranes during potentiometric measurements (spectropotentiometry) and image concentration profiles *in situ* with high spatial and temporal resolution. The combination of electrochemical and optical information helped to interpret non-idealities in the potentiometric responses, suppress or tailor the undesirable transport across sensor membranes, and estimate the residual lifetime of chronically implanted sensors. These novel opportunities provide feedback in membrane optimizations and are expected to lead to sensor systems with picomolar detection limits and superb selectivities.

INTRODUCTION

Discussions concerning the importance of interfacial ion exchange and membrane bulk diffusion processes dominated the debates on the origin of ion selectivity and the response mechanism of ion-selective electrodes (ISEs) [1–4]. Numerous intuitive experimental techniques have been developed for understanding the potential determining process [5–9]. Recently, the appearance of pH-sensitive chromoionophores [10] provided direct experimental evidence that the equilibrium partitioning of sample ions at the sample membrane interface is the main parameter governing the potentiometric response. Chromoionophores are selective complexing agents with intensive absorbance bands in the visible spectral range. The absorbance of the complexed (protonated) and free (deprotonated) ionophore is linearly related to the concentration of the respective species (Beer–Lambert law). Bakker determined the degree of protonation of the H^+ selective chromoionophore (ETH 2418) in 2-µm-thick pH-sensitive membrane optically and proved that the membrane composition remains constant in the Nernstian response range of ionophore-based sensors [7]. In very alkaline or acidic solutions, however, the degree of protonation changes due to the lack of ion selectivity or complete salt coextraction, respectively. The changes in the membrane composition corresponded perfectly with the deviations in the potentiometric response of a pH sensor, based on a membrane with the same composition.

In Bakker's experiment the directions of the optical observation and ion transport were the same, and, accordingly, the mean concentrations in the membrane cross-section were determined. The avail-

*Lecture presented at the 11th European Conference on Analytical Chemistry (EUROANALYSIS XI), Lisbon, Portugal, 3–9 September 2000. Other presentations are published in this issue, pp. 1–54.

†Corresponding author

ability of ion-selective chromoionophores has brought about additional possibilities in speciation and led to the development of a novel imaging method spectropotentiometry [11]. The essence of this technique is monitoring membrane component concentrations perpendicular to the direction of ion transport. This led to the visualization of the concentration gradients of the protonated and deprotonated forms of the ionophore across the membrane thickness. Spectropotentiometry has been designed to image the transport of species in the cross-section of ISE membranes, in parallel to real-time measurement of transient potentials. It has been used to follow the redistribution of membrane components in H^+-selective electrode membranes during cation [11] and anion [12] interference and to trace the water uptake under different experimental conditions [13]. The experimental findings are essential to understand equilibration processes, long-time drifts, and transient responses.

The first spectropotentiometric investigations were limited to pH-sensitive chromoionophores, and single wavelength measurements in the membrane bulk. Ion transport was established across the membrane by choosing an electrolyte on one side of the membrane with high concentration of interfering cations or anions. Lately, we extended the imaging experiments to the aqueous sides of the phase boundaries of H^+-selective membranes by adding bromochresol green indicator into the sample and following pH changes in the superficial layer due to H^+ ion transport. In addition, the single wavelength measurements have been replaced by multi wavelength, full-spectral imaging using a Prism and Reflector Imaging Spectroscopy System (PARISS) microspectrometer. The PARISS system acquires the complete spectra of all objects (compounds) in a "slice" of image simultaneously (240 spectral plots per acquisition). Finally, high-resolution images were recorded in current polarized membranes and in chronoamperometric experiments.

RESULTS AND DISCUSSIONS

The experimental set-up used to study the transport processes in ISE membranes in combination with potentiometric and chronoamperometric experiments is shown in Fig. 1. A thin-layer electrochemical cell is placed on the stage of an optical microscope, equipped with a PARISS imaging spectrometer. In the electrochemical (potentiometric) cell, the ion-selective membrane ring separates two solution com-

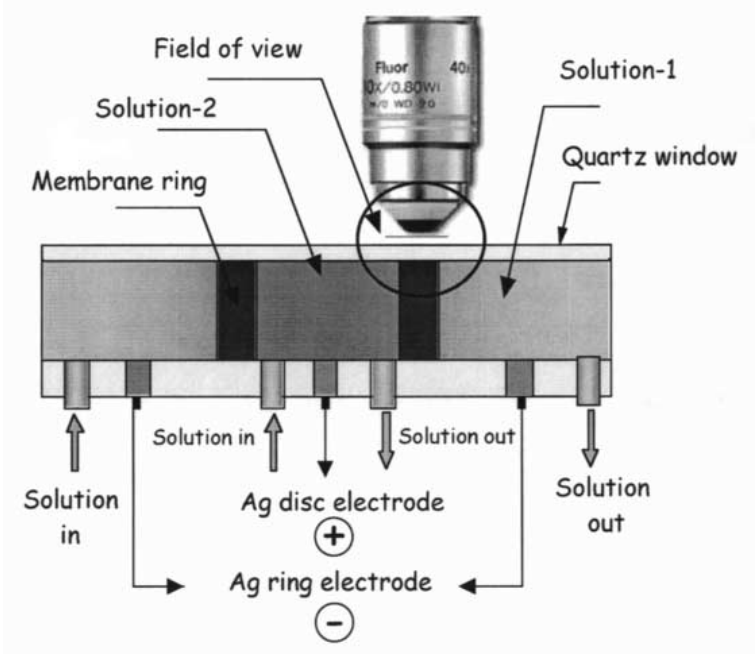

Fig. 1 Experimental set-up and thin-layer electrochemical cell for spectropotentiometric imaging.

partments, the inner filling solution (IFS), and the sample. There is a silver electrode in each compartment (a silver disc electrode in the inner compartment and a silver ring in the outer compartment). The imaging camera records 240 spectra in the visible range (from 400 to 800 nm) across the membrane simultaneously to potentiometric, chronoamperometric, or chronopotentiometric measurements. Using ion-selective chromoionophores the concentration profiles of the free and complexed ionophore are followed in time. In Fig. 2, the distribution of optically active compounds in an ETH 5294-based pH-sensitive membrane and the contacting solution are shown in a three-dimensional intensity image. To visualize pH changes in the solution phase, a bromochresol green indicator was added to the sample solution.

Most recent studies on transport phenomena in sensor membranes provided essential information on processes determining the apparent detection limit and selectivity of ion-selective electrodes. It was shown that infinitesimally small amounts of ions, leaching from the membrane, poise the phase boundary potential, and the detection limits could be extended from micromolar to nano- and picomolar concentrations in parallel to dramatic improvements in the sensor selectivities when this leaching was eliminated. Sokalski *et. al*. [14–16] applied a concentration gradient across the membrane, toward the IFS, to avoid the undesirable leaching. We showed [17] that galvanostatically controlled current can also be used to prevent ion leaching and to control ion transport through ion-selective membranes. Compared to the method of Sokalski, the electrochemical control of ionic fluxes [17] offers several advantages. The fine-tuning of the applied current is simple compared to the adjustment of concentration gradients induced cross fluxes. The current can be applied as short pulses or pulse trains, and unintended concentration polarization and resistance changes in the membrane can be restored/eliminated by reversing the direction of current. The best results were achieved when our current polarization method is applied in combination with minor concentration gradients in the opposite direction [18]. In this way, stable steady state conditions (ionic fluxes) can be reached with all the advantages of current polarization. The optimal setting of balanced ionic fluxes can be achieved by using the concentration images in the membrane cross-section and the calibration curve as feedback. During this delicate optimization our goal is

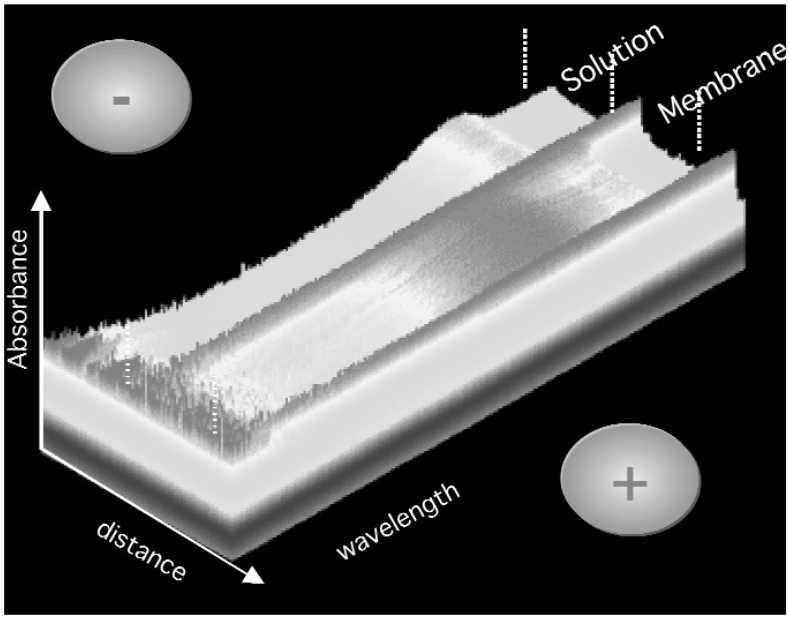

Fig. 2 Three-dimensional image of a pH selective membrane in contact with a pH = 6 phosphate buffer solution. The +/– sign marks the direction of current polarization. Dark areas show strong absorption bands of the chromoionophore (membrane phase) and the bromochresol green indicator (solution phase).

to establish horizontal, space-independent concentration profiles, claimed to be necessary for Nernstian response.

Figure 3 summarizes the spectral information collected with the imaging system. The upper left picture is the observed image of a section of the ring-shaped membrane. S and M mark the solution and membrane phase, respectively. The signs + and – indicate the polarity of the applied current. The marker line indicates the cross-section where the 240 spectra are collected. In the upper right corner, the color-codified intensity (in gray scale in Fig. 3) spectra of the membrane and the solution are shown. Dark areas mean small light intensity, strong absorption. The lower three pictures are absorption spectra collected at the positively or negatively polarized side of a phenoxazine derivative (ETH-5294, pH-sensitive chromoionophore) loaded membrane and in the solution, spiked with bromochresol green indicator dye, respectively.

When ions are transported through the membrane, e.g., due to lack of selectivity, the theoretical potentiometric response is compromised. The theoretical response can be restored when the leaching of ions is offset by tailored, current-controlled transport, i.e., the concentration profiles in the membrane are flat and space independent. Using the concentration images, the detection limits of current polarized calcium [17] and lead-selective electrodes [18] were extended to 5×10^{-10} and 10^{-11} M, respectively. These extended concentration ranges open new areas of application for ion sensors in biological and environmental analysis, e.g., intracellular ion activity measurements or continuous monitoring of heavy metal contaminants both in biological fluids or environmental analytes.

Spectral imaging is a powerful technique to identify, map, and quantify objects simultaneously in heterogeneous samples, captured in the field of view. It is used in a wide variety of applications ranging from Earth resource monitoring (in the latter case, a telescope replacing the microscope) to cytology and malignancy detection. When extremely small ion-sensors are used in continuous monitoring

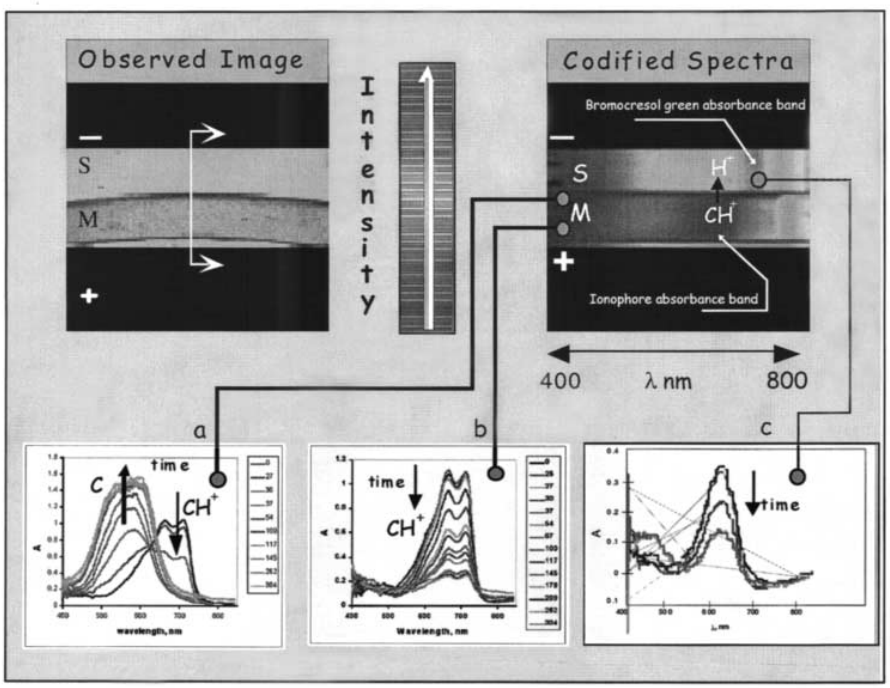

Fig. 3 Summary of spectral information collected with the spectropotentiometric setup. The +/- sign marks the direction of the polarizing current. S: solution; M: membrane; CH^+ and C: protonated and deprotonated chromoionophore.

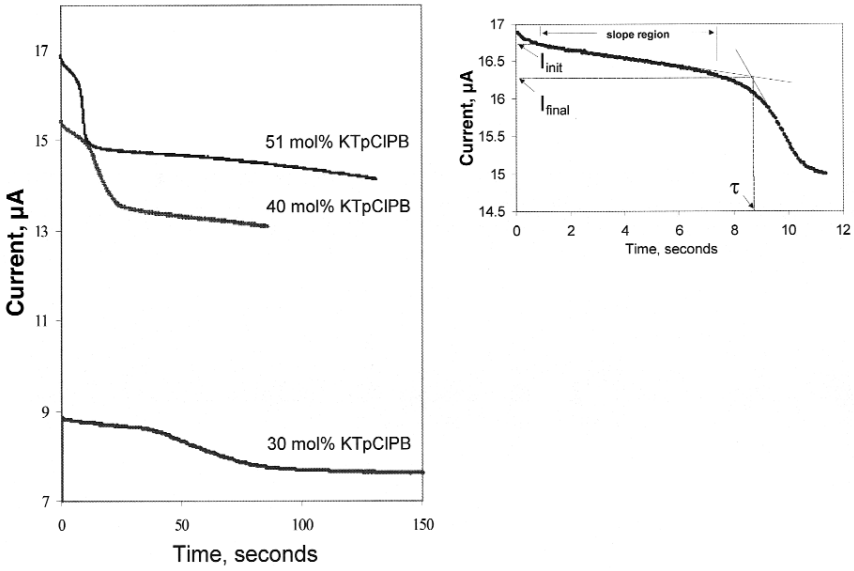

Fig. 4 Chronoamperometric current-time transients recorded with a valinomycin-containing mobile site membrane (left) and the evaluation of the slope, break time (τ), I_{init} and I_{final} values (right). The applied voltage (V_{appl}) was 4 V.

(chronically implanted devices and flow-through blood electrolyte analyzers) the loss of membrane ingredients (selective ionophore and lipophilic salt additive) into the sample is determining the long-term stability of the response and the lifetime of the sensor. Unfortunately, there is no possibility for precise calibration of chemical sensors implanted into the tissue. Using the concentration images recorded in current polarized membranes, we developed a novel chronoamperometric method (measuring the current-time transients after a voltage step is applied across the membrane) to estimate this loss, and to follow changes in the optimal membrane composition [19,20]. The method is appropriate to detect critical changes in the membrane composition of ISEs. Tracking these changes may have practical relevance in predicting the residual lifetime and minimizing the probability of false interpretation of sensor signals. The prediction of residual lifetime may also be important for clinical analyzers. It may signal special service prior to electrode failure. In Fig. 4 the chronoamperometric current-time transients of a valinomycin-based potassium-selective electrode are shown with varying amounts of potassium tetrakis(4-chlorophenyl)borate (KTpClPB).

The break time (τ) [21] and the experimentally determined slope [19] are proportional to the free ionophore concentration according to eqs. 1 and 2:

$$\tau^{1/2} = \frac{FA\left(C_{val} - C_{site}\right)\sqrt{D_{val}\pi}}{2I_{init}} \tag{1}$$

$$slope = \frac{4(I_{final} - I_{init})}{F^2 A^2 D_{val}\pi} \cdot \frac{I_{init}^2}{\left(C_{val} - C_{site}\right)^2} \tag{2}$$

where τ is the break time in the current transient, A is the membrane area, F is the Faraday constant, C_{val} and C_{site} are the free ionophore, and the negatively charged site concentration in the membrane, D_{val} is the diffusion coefficient of the ionophore, I_{init} and I_{final} are current values at the transients (explanation is given in Fig. 4), $I_{init}=V_{appl}/R_{ohm}$ where R_{ohm} is the ohmic resistance of the membrane and V_{appl} is the

applied voltage. The ohmic resistance of the membrane is primarily determined by the mobile site concentration [8]:

$$R_{ohm} = \frac{V_{appl}}{I_{init}} = \frac{RTd}{2AF^2 C_{site}(D_{Kval^+} + D_{site})} \quad (3)$$

Equations 1 and 2 provide means of assessing the free ionophore concentration in the membrane while the residual C_{site} concentration can be determined with the help of eq. 3. Imaging the membrane cross-section during the chronoamperometric measurements proved that the break time appears when the free ionophore is completely depleted at one side of the membrane.

Our ultimate goal is to utilize this chronoamperometric method for sensor diagnostic to evaluate the conditions of chronically implanted ISE membranes. The current time curves of planar, microfabricated ISEs showed the same characteristics features as described above. When the free ionophore and site concentrations were determined from the calibration plots based on eqs. 1–3 they were in ±10% agreement with the known membrane formulation.

ACKNOWLEDGMENT

The financial support of the FRG grant 2-22307 of the University of Memphis is gratefully acknowledged.

REFERENCES

1. W. E. Morf and W. Simon. *Helv. Chim. Acta* **69**, 1120 (1986).
2. R. P. Buck, T. M. Nahir, V. V. Cosofret, E. Lindner, M. Erdôsy. *Anal. Proc.* **31**, 301 (1994).
3. R. P. Buck and E. Lindner. *Accounts for Chemical Research* **31**, 257 (1998).
4. E. Pungor. *Electroanalysis* **8**, 348 (1996).
5. A. P. Thoma, A. Viviani-Naurer, S. Arvanitis, W. E. Morf, W. Simon. *Anal. Chem.* **49**, 1567 (1977).
6. E. Lindner, K. Tóth, E. Pungor, T. R. Berube, R. P. Buck. *Anal. Chem.* **59**, 2213 (1987).
7. E. Bakker, M. Nägel, U. Schaller, E. Pretsch. *Electroanalysis* **7**, 817 (1995).
8. T. M. Nahir and R. P. Buck. *J. Phys. Chem.* **97**, 12363 (1993).
9. K. Tohda, Y. Umezawa, S. Yoshiyagawa, S. Hashimoto, M. Kawasaki. *Anal. Chem.* **67**, 570 (1995).
10. E. Bakker, M. Lerchi, T. Rosatzin, B. Rusterholz, W. Simon. *Anal. Chim. Acta* **278**, 211 (1993).
11. B. Schneider, T. Zwickl, B. Federer, E. Pretsch, E. Lindner. *Anal. Chem.* **68**, 4342 (1996).
12. E. Lindner, T. Zwickl, E. Bakker, B. T. T. Lan, K. Tóth, E. Pretsch. *Anal. Chem.* **70**, 1176 (1998).
13. T. Zwickl, B. Schneider, E. Lindner, T. Sokalski, U. Schaller, E. Pretsch. *Anal. Sci.* **14**, 57 (1998).
14. T. Sokalski, A. Ceresa, T. Zwickl, E. Pretsch. *J. Am. Chem. Soc.* **119**, 11347 (1997).
15. T. Sokalski, T. Zwickl, E. Bakker, E. Pretsch. *Anal. Chem.* **71**, 1204 (1999).
16. T. Sokalski, A. Ceresa, M. Fibbioli, T. Zwickl, E. Bakker, E. Pretsch. *Anal. Chem.* **71**, 1210 (1999).
17. E. Lindner, R. E. Gyurcsanyi, R. P. Buck. *Electroanalysis* **11**, 695 (1999).
18. E. Pergel, R. E. Gyurcsányi, K. Toth, E. Lindner. *Anal. Chem*. (2001), submitted for publication.
19. B. D. Pendley, E. Lindner, R. E. Gyurcsanyi, R. P. Buck. *Anal. Chem.* (2000), Submitted for publication.
20. B. D. Pendley and E. Lindner. *Anal. Chem.* **71**, 3673 (1999).
21. M. L. Iglehart, R. P. Buck, G. Horvai, E. Pungor. *Anal. Chem.* **60**, 1018 (1988).